Chemical Papers
https://doi.org/10.1007/s11696-019-00714-z

ORIGINAL PAPER

Prototypical *cis*-ruthenium(II) complexes present differential fluorescent staining in walled-cell models (yeasts)

Alexander Carreño[1,2] · Dayán Páez-Hernández[1] · César Zúñiga[1] · Angélica Ramírez-Osorio[2] · Jan Nevermann[3] · María Macarena Rivera-Zaldívar[3] · Carolina Otero[4] · Juan A. Fuentes[3]

Received: 14 December 2018 / Accepted: 6 February 2019

Abstract

cis-Ru(**deeb**)$_3^{2+}$ (**R1**; where **deeb** is 4,4′-diethanoate-2,2′-bipyridine) and *cis*-Ru(**phen**)$_3^{2+}$ (**R2**; where **phen** is 1,10-phenanthroline) were synthesized. Although the presence of the cell wall (a structure that is present in yeasts and bacteria,) was previously described as a natural barrier that hampers the uptake of d^6-based luminescent complexes, we previously demonstrated that rhenium(I) tricarbonyl complexes were useful to stain both yeasts and bacteria. Even though several studies of classical ruthenium(II) complexes can be found, none of those studies aimed to determine the potential of these compounds as biomarkers for walled cells, testing only cell lines that lack this permeability barrier. Walled cells exhibit a relatively rigid structure, mainly constituted by carbohydrates and proteins, and surround the plasma membrane. In this manuscript, we observed that both **R1** and **R2** exhibited very low cytotoxicity in different walled-cell models (including bacteria and yeasts). More importantly, we found that both **R1** and **R2** were able to fluorescently stain *Candida albicans* (yeast), with a simple and fast procedure, without the need of additional permeabilizer molecules and antibodies. Interestingly, **R1** remained retained in a discrete central structure consistent with the cell nucleus, whereas **R2** seemed to be accumulated in the cell wall. These results show that these two complexes can be used as biomarkers for walled cells as differential staining, supporting the fact that, as well as with rhenium(I) complexes, biomarkers properties can be modulated by changing the substituents in ruthenium(II)-derivative luminescent stains, even for walled cells.

Keywords Ruthenium(II) complexes · Spin–orbit DFT · Cytotoxicity · Biomarkers · Yeasts

Electronic supplementary material The online version of this article (https://doi.org/10.1007/s11696-019-00714-z) contains supplementary material, which is available to authorized users.

✉ Alexander Carreño
alexander.carreno@unab.cl
http://www.cans.cl

✉ Dayán Páez-Hernández
dayan.paez@unab.cl
http://www.cans.cl

✉ Juan A. Fuentes
jfuentes@unab.cl

[1] Center of Applied Nanoscience (CANS), Universidad Andres Bello, República 275, Santiago, Chile

[2] Fondo Nacional de Desarrollo Científico y Tecnológico (FONDECYT 11170637), Santiago, Chile

[3] Laboratorio de Genética y Patogénesis Bacteriana, Facultad de Ciencias de la Vida, Universidad Andrés Bello, República 330, Santiago, Chile

[4] Escuela de Química y Farmacia, Facultad de Medicina, Universidad Andres Bello, Santiago, Chile

Introduction

Research of ruthenium(II) nitrogenated complexes have received interest as photosensitizers in dye solar cells (DSSC) application due to their favorable photoelectrochemical properties and high stability in the oxidized state (Bomben et al. 2010; Caramori et al. 2010; Nazeeruddin et al. 2001; Oßwald et al. 2017; Sampaio et al. 2017; Zhong et al. 2011). Development of ruthenium(II) complexes of type *cis*-ruthenium(II) (***N***,***N***)$_3^{2+}$, where ***N***,***N*** is a dinitrogenated ligand such as 2,2′-bipyridine or 1,10-phenanthroline derivatives, or monodentated such as halogens or −SCN, among others, dates to the 1990s (Bignozzi et al. 1993; Bonhote et al. 1999; Juris et al. 1988). These complexes have been described as useful in high efficiency in the conversion of high incident solar light into electricity, mainly due to their wide absorption range from the visible light to the near infrared (NIR) adsorption (Katsumata et al. 2017; Koyyada et al. 2016; Sauvage et al. 1994). The absorption spectra

Published online: 15 March 2019

of ruthenium(II) dinitrogenated compounds can be modulated according to the nature of their ligands, including the HOMO and LUMO energy levels (Al-Noaimi and AlDamen 2012; Li et al. 2014; Sacksteder et al. 1990; Sangilipandi et al. 2016; Song et al. 2017).

Normally, ruthenium(II) polypyridyl complexes have been described as possible anticancer agents (Poynton et al. 2017), including Ru(II) cyclometallated complexes (Biancalana et al. 2017). Interestingly, intracellular localization of Ru(II)-based complexes has been monitored by confocal microscopy, showing that these complexes are normally retained in the cell nucleus in non-walled cells (e.g., epithelial cells). These findings are consistent with the previously described DNA-disrupting activity of some Ru(II) complexes (Li et al. 2015; Schatzschneider 2018). The use of confocal microscopy, which allows obtaining images through the *Z* axis, has also remarked an alternative use of Ru(II) complexes as cellular biomarkers (Byrne et al. 2016). Nevertheless, Ru(II)-based biomarkers have been exclusively tested in non-walled eukaryotic cells (e.g, baby hamster kidney cells BHK, human embryonic kidney cells HEK-293, and liver carcinoma HEp-G2) (Li et al. 2015), where their potential use as biomarkers have not been assessed in walled cells such as bacteria (prokaryotic) and yeasts (fungi, eukaryotic). Both bacteria and fungi (yeasts) exhibit a rigid structure in their envelop, called cell wall (Caveney et al. 2018; Sanz et al. 2017). Although these structures are not chemically related in these two biological groups, in both cases, the presence of a cell wall could hamper the uptake of foreign molecules, including biomarkers. In this context, bacteria and fungi are considered as "walled cells", since these cell types harbor a cell wall, whereas epithelial cells are "non-walled cells" because they lack this structure. In fact, it has been stated that, at least for Re(I) tricarbonyl complexes, the presence of the cell wall can be considered as a barrier that impairs the uptake of biomarkers (Amoroso et al. 2007). However, we reported that the use of monocationic Re(I) tricarbonyl complexes with suitable ancillary ligands allows an enough uptake to permit their use as biomarkers in walled cells, including bacteria and yeasts (Carreno et al. 2016b, 2017b, c). Thus, we wondered whether Ru(II) complexes, substituted with different dinitrogenated ligands (i.e. 2,2′-bipyridine or 1,10-phenanthroline), are suitable as biomarkers in walled cell such as bacteria (Gram-negative bacteria: *Salmonella enterica*; Gram-positive bacteria: *Staphylococcus aureus* and *Bacillus cereus*) and yeasts (*Candida albicans* and *Cryptococcus* spp.). For that aim, we synthesized two prototypical *cis*-Ruthenium(II)($\boldsymbol{N}$,$\boldsymbol{N}$)$_3^{2+}$ complexes (Wang et al. 2016; Zhou et al. 2005): *cis*-Ru(**deeb**)$_3^{2+}$ (**R1**; where **deeb** is 4,4′-diethanoate-2,2′-bipyridine) and *cis*-Ru(**phen**)$_3^{2+}$ (**R2**; where **phen** is 1,10-phenanthroline) (Scheme 1). In this context, the focus of the present study was not the full chemical characterization of either **R1** or **R2**, but the determination of their potential properties as biomarkers for walled-cell models. In addition, to better understand the emission of these compounds, we performed a relativistic computational protocol to explore not only the nature and assignment of the transition but also the possible mechanism. It is necessary to consider the relativistic effects and, particularly, the role of the spin–orbit coupling because it determines the amount of different spin-free multiplicities involved in the emission process (Carreno et al. 2019; Rojas-Poblete et al. 2018). In addition, we performed assays to determine the potential cytotoxicity of both **R1** and **R2** in different cell models, including bacteria (walled prokaryotic cells) and yeasts (walled eukaryotic cells).

Regarding the potential as biomarkers in walled cells, we found that both **R1** and **R2** efficiently stained yeasts, including *Candida albicans* and *Cryptococcus* spp. with a simple and fast procedure, without the need of additional permeabilizer molecules and antibodies. Interestingly, **R1** and **R2** exhibited differential staining patterns, where **R1** specifically was retained in a central structure that could be interpreted as the nucleus, and **R2** stained a peripheric structure that could correspond to the cell wall. In

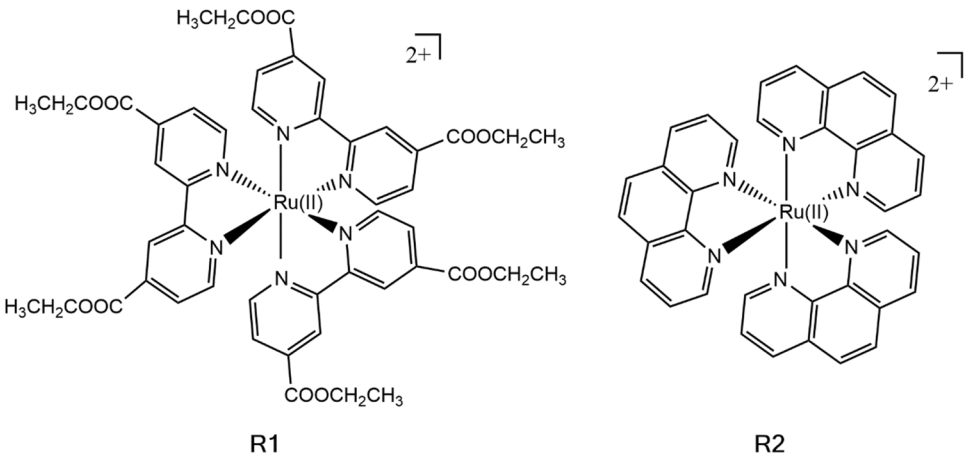

Scheme 1 Chemical structure of the ligands **deeb** (4,4′-diethanoate-2,2′-bipyridine), and **phen** (1,10-phenanthroline); and the *cis*-ruthenium(II)($\boldsymbol{N}$,$\boldsymbol{N}$)$_3^{2+}$ complexes **R1** (*cis*-Ru(**deeb**)$_3^{2+}$) and **R2** (*cis*-Ru(**phen**)$_3^{2+}$)

summary, we showed that *cis*-Ruthenium(II)$(N,N)_3^{2+}$ complexes present properties as suitable biomarkers for walled cells in a simple and fast procedure, without the need of additional permeabilized molecules and antibodies.

Quantum chemistry calculations

All calculations reported here were carried out in the framework of the density functional theory (DFT) using the Amsterdam Density Functional computational package (ADF) via the zeroth-order regular approximation (ZORA) Hamiltonian, including spin–orbit (SO) relativistic corrections and Slater Type Orbitals (STO) basis sets with triple–ζ accuracy plus double polarization function (TZ2P) for all the atoms (Muñoz-Castro et al. 2017). The molecular geometry of the ground states was fully optimized via GGA-BP86 functional (Averkiev et al. 2014; Micciarelli et al. 2017). In all cases, frequency analysis was performed after each geometry optimization, where we obtained only positive frequencies verifying the local minima. Time-dependent DFT (TDDFT) was used to determine the origin of the emission of the complexes and to assign the transitions (Yang et al. 2006; Zarate et al. 2013). Since calculations use the physical meaning of phosphorescence, a previously known excitation wavelength is not necessary to obtain the theoretical emission (Macleod-Carey et al. 2018). Solvation effects were considered via the conductor-like screening model (COSMO) using acetonitrile as solvent (Sinnecker et al. 2006; Sistla and Khanna 2011). More detailed calculations were performed by the self-consistent two-component spin–orbit coupling TDDFT (SOC-TDDFT) within the ZORA Hamiltonian (Fantacci et al. 2005; Grotjahn et al. 2017). ADF allowed us to better estimate the emission wavelength. In all cases, at least five spin-mixed excitations were calculated in the full SOC-TDDFT calculations (Franco de Carvalho et al. 2017; Grotjahn et al. 2017; Páez-Hernández et al. 2012; Younker and Dobbs 2013). It is important to remark that, in a non-relativistic framework, spin functions can be classified depending on the spin-projection quantum number (m_s) as $\alpha = |1/2,1/2>$ and $\beta = |1/2,-1/2>$ functions. When spin–orbit coupling is included in the calculations, the spin is no longer a good quantum number, and α and β functions mix between them. In this scenario, all these effects are treated at scalar relativistic time-dependent density functional theory with ZORA Hamiltonian (SR-TDDFT/ZORA) (Weerawardene and Aikens 2018; Zalis et al. 2015) and spin–orbit time-dependent density functional theory with ZORA Hamiltonian (SO-TDDFT/ZORA) (Van Kuiken et al. 2013).

Experimental

All starting materials and solvents were purchased from Merck and Aldrich and used with no further purification. The purity of each compound (**deeb**, **R1** and **R2**) was checked by ^{1}H NMR recorded on a Bruker AVANCE 400 spectrometer at 400 MHz at 25 °C. Samples were dissolved in deuterated DMSO (for R1 and R2), or chloroform (for deeb). In all the cases, we used tetramethylsilane as an internal reference.

Antimicrobial activity

Both **R1** and **R2** complexes were evaluated for their in vitro growth inhibitory activity against the clinical yeasts *Candida albicans* and *Cryptococcus* spp., obtained from the Hospital Clínico of the Universidad de Chile, Santiago, Chile; the Gram-negative pathogen *Salmonella enterica* serovar Typhimurium ATCC14028s; the Gram-positive pathogen *Staphylococcus aureus*; and the sporulated Gram-positive *Bacillus cereus* obtained from the Hospital Clínico of the Universidad de Chile, Santiago, Chile. Minimum inhibitory concentration (MIC) was obtained by broth dilution as described (Cuenca-Estrella et al. 2003). The MIC is defined as the lowest concentration of the tested compounds at which no growth of the strain was observed after the incubation (Cuenca-Estrella et al. 2003). Yeasts were previously cultured in Sabouraud agar (Bacto peptone, 10 g/L; glucose, 40 g/L; agar, 15 g/L; pH 5.6) at 28 °C. Bacteria were previously cultured in Luria–Bertani broth (Bacto peptone, 10 g/L; NaCl, 5.0 g/L; peptone, 10 g/L; yeast extract 10 g/L). Further dilutions of microorganisms (0.5 McFarland) were performed with Bacto Tryptic Soy broth (pancreatic digest casein 17.0 g/L, papaic digest of soybean 3.0 g/L, dextrose 2.5 g/L, sodium chloride 5.0 g/L, dipotassium phosphate 2.5 g/L). Stock solutions of the tested compounds were prepared in dimethyl sulfoxide (DMSO). The inoculated wells were then incubated at 28 °C (yeasts) or 37 °C (bacteria) for 24, 48 and 72 h. The MIC values of the tested compounds were obtained as mM. All the experiments were performed in biological triplicate, each in technical triplicate.

Fluorescence microscopy studies

Bacteria (*Salmonella enterica* serovar Typhimurium ATCC14028s, *Staphylococcus aureus*, and *Bacillus cereus*) were grown 24 h at 37 °C in Luria–Bertani plates (Bacto peptone, 10 g/L; NaCl, 5.0 g/L; peptone, 10 g/L; yeast extract 10 g/L; agar 15 g/L). Yeasts (*Candida albicans* and

Cryptococcus spp.) were grown 48 h at 28 °C in Sabouraud agar. For staining, either bacteria or yeasts (approximately 10^9 cfu/ml) were washed twice and resuspended in one volume of phosphate buffer solution (PBS). The microorganisms were mixed with either **R1** or **R2** (2 mM as final concentration, 40% v/v or 5.6 M DMSO), incubated 90 min at 37 °C and subsequently washed three times with PBS to remove the excess of unbound complexes. It has been stated that the DMSO is a relatively innocuous solvent for yeasts, at least at 6 M (Chaves and da Silva 2012; León-García et al. 2017; Westwater et al. 2005). Finally, microorganisms were resuspended in one volume of PBS prior to being immobilized with 1% agarose in PBS and observed at 1000 × (100 × objective, 10 × ocular, NA 1.4, with immersion oil 1.510) with confocal microscopy (Leica MicroSystems). Since yeasts present autofluorescence, we set detection threshold (fluorescence emission was obtained by laser excitation at 405 nm with 20% power intensity) using yeasts treated with DMSO alone (Carreno et al. 2016a). Emission was collected with a long-pass emission filter in the range of 450–727 nm. To avoid photobleaching, samples were photographed before 5 min of exposure under the microscope.

Materials

The synthetic procedure to obtain the ligand, **R1** and **R2** complexes, was reported in literature (Donnici et al. 1998).

Synthesis of 4,4′-diethanoate-2,2′-bipyridine (deeb)

This compound was prepared by reaction of 4,4′-dicarboxy-2,2′-bipyridine in a mixture of sulfuric acid and absolute ethanol according a published procedure (Donnici et al. 1998). Yield 60%. ^{1}H NMR (400 MHz, chloroform-$_d$, 7.24 ppm): 8.92 (d, 2H); 8.86 (d, 2H); 7.91 (dd, 2H); 4.45 (quartet, –CH_2–), 1.44 (*t*, –CH_3).

Synthesis of *cis*-ruthenium(II) $(deeb)_3(PF_6)_2$ (R1)

We dissolved $RuCl_3 \times H_2O$ (0.22 mmol), and hydroquinone (0.65 mmol) in 25 ml of ethanol. Then, add **deeb** (0.71 mmol) and reflux with stirring in the dark, and under nitrogen atmosphere for 24 h. The mixture was cooled to room temperature and add 0.1 g of NH_4PF_6 and stirring for 24 h. The precipitate was filtered, washed with petroleum ether, and vacuum-dried, to obtain an orange powder (Zhou et al. 2005). Yield 50%. ^{1}H NMR (400 MHz, DMSO-$_{d6}$, 2.50 ppm); 9.33 (s, 2H), 7.96 (d, 2H), 7.84 (d, 2H), 4.43 (quartet, –CH_2–), 1.34 (*t*, –CH_3).

Synthesis of *cis*-ruthenium(II) $(phen)_3(PF_6)_2$ (R2)

The procedure was similar to that described for **R1**. The orange-light precipitate was filtered, washed with ethanol and diethyl ether. Yield 63%. ^{1}H NMR (400 MHz, $DMSO_{d6}$, 2.50 ppm); 8.77 (d, 2H), 8.39 (s, 2H), 8.09 (d, 2H), 7.77 (dd, 2H) (Wang et al. 2016).

Results and discussion

Experimental and theoretical calculations

The 4,4′-diethanoate-2,2′-bipyridine (**deeb**) ligand was synthesized from the 4,4′-dicarboxylic-2,2′-bipyridine acid, as previously reported (Donnici et al. 1998). **R1** and **R2** were synthesized by a traditional route involving the reaction of the corresponding dinitrogenated ligand (**deeb** or **phen**) with ruthenium(III) at reflux under inert atmosphere in the dark, to obtain the more stable *cis*-ruthenium(II) complexes (Dreyse et al. 2013; Gajardo et al. 2011). The complexes were precipitated by adding PF_6^- and recrystallized from ethanol/diethyl ether (2:1) with a good yield. Both structure and purity of complexes were corroborated by ^{1}H NMR (see Figures S1, S2 and S3 in the ESI†) (Tsai and Chang 2017; Wang et al. 2016; Zhou et al. 2005).

Both **R1** and **R2** have been previously characterized, including theoretical studies. Nevertheless, the optical properties of these complexes, a very relevant aspect considering their potential use as biomarkers, have not been previously addressed in depth. In this context, we performed calculations using SOC-TDDFT level of theory, including relativistic effects to describe electronic transitions in terms of the molecular spinors. For both complexes, the emission has a LMCT character and can be assigned as $\pi^* \rightarrow$ d transition. For **R1**, the emission band is centered at 633 nm and, for **R2,** at 688 nm. These values agree with the experimental reports for these systems (Ardo et al. 2010; Farnum et al. 2012; Favereau et al. 2016). We also calculated the emission lifetime, which was 1.4×10^{-5} s and 2.2×10^{-5} s for **R1** and **R2**, respectively, suggesting that the emission mechanism is phosphorescence in both cases. The nature of states involved in the emission corroborates this assertion because we found that, in both complexes, the spin-free triplet state contributes with 95% to the emissive state. In this case, it is important to underline that the normal selection rules, which forbid the spin flip transitions, need a reformulation when the spin–orbit interaction is considered. The molecular spinors have a contribution of both kinds of spin functions, $|\alpha>$ and $|\beta>$, and due to that the spin flip transitions are allowed in these cases. In our case, we consider both situations, SR-TDDFT/ZORA and SO-TDDFT/ZORA levels (Casida 2009), of calculations to describe the emission spectra of

both **R1** and **R2** (data not shown). **Figure 1** shows molecular orbitals involved in the emission of **R1**. The peripheral substituents were demitted during the optimization to avoid convergence problems due to their rotation.

Cytotoxicity assays of R1 and R2

As a first approach to determine the biological activity, we determined the cytotoxicity of **R1** and **R2** in different cell models. For this aim, we tested bacteria (prokaryotic walled cells), including Gram-negative (*Salmonella enterica* serovar Typhimurium ATCC14028 s), Gram-positive (*Staphylococcus aureus*), and sporulated Gram-positive (*Bacillus cereus*) strains, as well as yeasts (eukaryotic walled cells), including *Candida albicans* and the capsulated yeast, *Cryptococcus* spp. We observed that, in all cases, both **R1** and **R2** exerted no cytotoxic effect under the tested conditions. The only noticeable effect was observed with *Cryptococcus* spp., where both **R1** and **R2** presented a slight fungistatic effect only at 24 h of incubation (see Figure S4 in the ESI†). The fungistatic effect could be attributed to a fungal physiological adaptation and/or to a decrease effective concentration of compounds due to the presence of enzymes and other biomolecules that might modify the Ru complexes. Nevertheless, this effect disappears after 48 h. These results show that, both **R1** and **R2** exert low cytotoxicity, undistinguishable from the vehicle (DMSO) alone.

Confocal microscopy

Previously, confocal microscopy has allowed determining that dicationic Ru(II) polypyridyl complexes are retained in the nucleus of non-walled eukaryotic cells (Li et al. 2015; Schatzschneider 2018), presumably due to a possible interaction of the phosphate DNA groups with the positive charge of Ru(II) complexes. In addition, the planar symmetry of this kind of complexes could be also contributing to the interaction with DNA, as previously reported (Wu et al. 2018). Nevertheless, and as stated above, Ru(II)-based biomarkers have been exclusively tested in non-walled eukaryotic cells (Li et al. 2015). Considering that the presence of the cell wall plausibly could impair the uptake of foreign complexes, as previously suggested for monocationic Re(I) tricarbonyl complexes (Amoroso et al. 2007, 2008), we tested both **R1** and **R2** as biomarkers with the same cell models described above. Regarding bacteria, we found that both **R1** and **R2** were unable to reveal the presence of cells under the tested conditions (data not shown). By contrast, we observed that both **R1** and **R2** were suitable to stain yeasts, including both *Candida albicans* (Fig. 2) and *Cryptococcus* spp. (see Figure S5 in the ESI†), although these complexes seem to be more suitable for *Candida albicans*. The difference found between bacteria and fungi could be explained by a deficient uptake, due to the presence of a bacterial cell wall chemically different from the fungal cell wall (Gow et al. 2017; Yadav et al. 2018). In this case, bacterial cell wall could be hampering the uptake of complexes. Alternatively, it is also possible that the **R1** and/or **R2** are/is able to enter bacteria, but they are unable to remain retained inside cells after washing with phosphate buffer saline. Previously, similar results were reported with rhenium(I)-based complexes, which were suitable as biomarkers only for yeasts, but not for bacteria (Carreño et al. 2017a).

Our results showed that **R1** presented a discrete distribution inside cells, suggesting that this complex remained retained in the nucleus. This result is consistent with the previously reported data showing that Ru(II) complexes are retained in the nucleus of non-walled cells (e.g,. epithelial cells) (Li et al. 2015). Nevertheless, it is important to remark that this is the first report, to our knowledge, showing that ruthenium-based compounds might be as useful as biomarkers for walled cells, opening new applications for this kind of complexes. Interestingly, when **R2** was tested, we also observed a positive staining, but with a completely different pattern. At a first sight, we realized that **R2** apparently stained the whole cell, marking a sharp difference with the

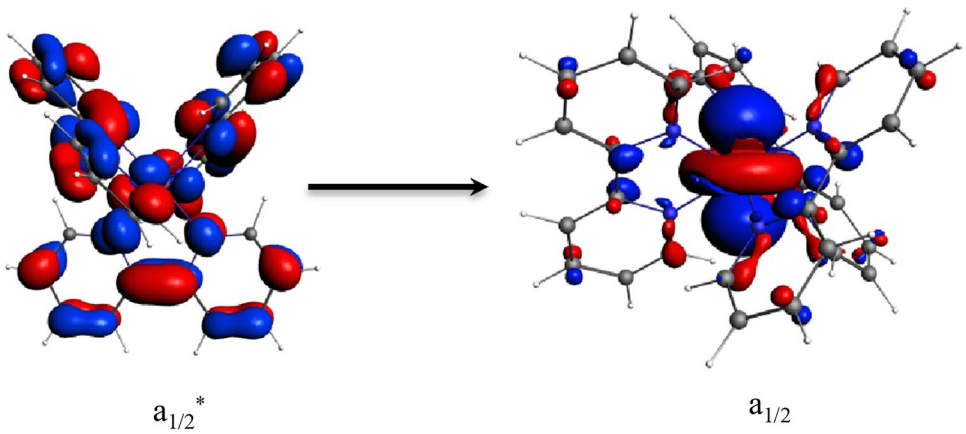

Fig. 1 Molecular orbitals involved in the emission of **R1** (similar to **R2**). The $a_{1/2*}$ represents the A irrep (group theory) in the double-value group representation. $a_{1/2}$ corresponds to the spin notation

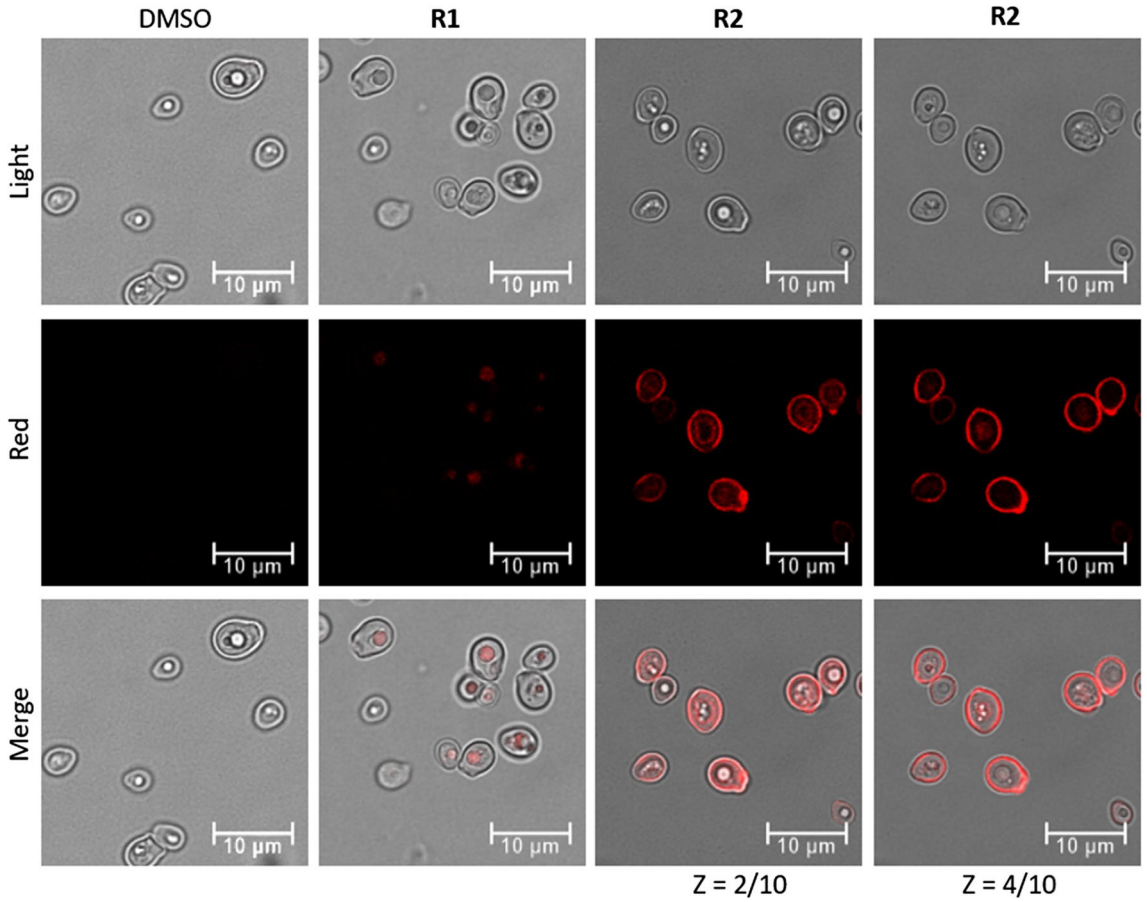

Fig. 2 Fluorescence confocal microscopy images showing *Candida albicans* (yeast). The "Red channel" corresponded to excitation of 405 nm and emission collected in a range of 450–727 nm. In all cases, microorganisms were observed fresh, immobilized with 1% agarose, using ×1000. DMSO alone was used to set the detection threshold. The *Z* axis was divided into 10 confocal slices. Images obtained for **R2** show two confocal slices (2 and 4, respectively)

results obtained with **R1** (Fig. 2, see $Z = 2/10$). However, taking advantage of the confocal microscopy, a technique that allows observing different focal fields through the *Z* axis, we analyzed images in more detail. When we observed the same images in a different slice, we realized that **R2** was retained in a structure that surrounds the cell (Fig. 2, see $Z = 4/10$). Considering the thickness of the stained structure, we speculate that **R2** could be useful to specifically stain the cell wall. In this case, we speculate that the differential cell localization of **R1** and **R2** can be attributed to the chemical nature of these two complexes. In **R1**, ruthenium(II) is coordinated with three substituted 2,2′-bipyridine moieties, whereas in **R2**, ruthenium(II) is coordinated with three 1,10-phenanthroline moieties (Scheme 1). Since 2,2′-bipyridine moieties present ethyl ester, a polar substituent, and 1,10-phenanthroline are constituted by three fused aromatic rings, without polar substituents, the possibility of interactions via hydrogen bonds through carbonyls in **R1** is higher compared to **R2**. It has been reported that both DNA and proteins, two biomolecules highly abundant in the nucleus, are able to interact with exogenous molecules via hydrogen bonds (Rowe and Ho 2017), explaining why **R1** is apparently retained in the cell compartment. On the other hand, **R2** does not present functional groups able to form hydrogen bonds, where only Van der Waals interactions are likely possible. In the case of **R2**, it is possible that Van der Waals interactions contributed to retain the complex in structures found in the cells surface, such as the cell wall (Kendall and Roberts 2015; Nir and Andersen 1977). Nevertheless, more experimentation is needed to fully understand the molecular mechanisms underlaying the differential staining between **R1** and **R2**.

It is important to remark that our staining protocol can be performed without the need of additional permeabilization steps. In this sense, DMSO has been known to enhance cell membrane permeability of drugs or DNA, at least in unwalled cells (i.e., epithelial cell line) (de Menorval et al. 2012). Nevertheless, we want to underline that, when we tested other fluorescent, d^6-metal complexes with this same staining protocol, we were unable to obtain an efficient

staining, indicating that the mere presence of DMSO does not assure a successful result in this king of biomarkers (Carreño et al. 2017a).

Altogether, these results show that Ru(II)-based complexes might be useful to develop new biomarkers for walled cells such as yeasts, similar to other Re(I)-based studies (Carreno et al. 2016b; Carreño et al. 2017b).

Conclusions

As determined by our relativistic DFT studies, both **R1** and **R2** exhibit a similar emission of ligand–metal charge transfer (LMCT) character. In addition, these complexes showed very low cytotoxicity against different cell models, including bacteria and yeasts. Regarding the biomarker potential, since **R1** and **R2** presented different staining pattern in yeasts, we concluded that changes in the substituents of the dinitrogenated ligands can be used to modulate biomarker properties of these kind of Ru(II) complexes, even for walled cells. These results show that these two complexes could be used as biomarkers for walled cells as luminescent staining. To our knowledge, this is the first report showing that ruthenium(II) complexes can be used as biomarkers for walled cells.

Acknowledgements We thank FONDECYT 11170637, 1181638, and 1180017. We thank Dr, Ramiro Arratia-Pérez (Center of Applied Nanoscience, Universidad Andres Bello) for the Computational Resources Facilities and Dr. Ivonne Chávez M (Departamento de Química Inorgánica, Pontificia Universidad Católica de Chile) for instrumental facilities.

Compliance with ethical standards

Conflicts of interest The authors declare no conflicts of interest.

Dedication This manuscript is dedicated to Professor Dr. Ramiro Arratia-Pérez (UNAB, director of Center of Applied Nanoscience, Chile), for his relevant contributions to the relativistic quantum chemistry in Chile, where he founded the first Molecular Relativistic School in Latin America, and in the world.

References

Al-Noaimi M, AlDamen MA (2012) Ruthenium complexes incorporating azoimine and α-diamine based ligands: synthesis, crystal structure, electrochemistry and DFT calculation. Inorg Chim Acta 387:45–51. https://doi.org/10.1016/j.ica.2011.12.050

Amoroso AJ et al (2007) Rhenium *fac* tricarbonyl bisimine complexes: biologically useful fluorochromes for cell imaging applications. Chem Commun. https://doi.org/10.1039/b706657k

Amoroso AJ et al (2008) 3-Chloromethylpyridyl bipyridine fac-tricarbonyl rhenium: a thiol-reactive luminophore for fluorescence microscopy accumulates in mitochondria. New J Chem 32:1097–1102. https://doi.org/10.1039/b802215a

Ardo S, Sun Y, Staniszewski A, Castellano FN, Meyer GJ (2010) Stark effects after excited-state interfacial electron transfer at sensitized TiO(2) nanocrystallites. J Am Chem Soc 132:6696–6709. https://doi.org/10.1021/ja909781g

Averkiev BB, Dreger ZA, Chaudhuri S (2014) Density functional theory calculations of pressure effects on the structure and vibrations of 1,1-diamino-2,2-dinitroethene (FOX-7). J Phys Chem A 118:10002–10010. https://doi.org/10.1021/jp508869n

Biancalana L, Pampaloni G, Marchetti F (2017) Arene ruthenium(II) complexes with phosphorous ligands as possible anticancer agents. Chimia 71:573–579. https://doi.org/10.2533/chimia.2017.573

Bignozzi CA, Chiorboli C, Murtaza Z, Jones WE, Meyer TJ (1993) Photophysical and photochemical behavior of nitro complexes of ruthenium(Ii). Inorg Chem 32:1036–1038. https://doi.org/10.1021/ic00058a047

Bomben PG, Koivisto BD, Berlinguette CP (2010) Cyclometalated Ru complexes of type [Ru(II)(N–N)(2)(C–N)](z): physicochemical response to substituents installed on the anionic ligand. Inorg Chem 49:4960–4971. https://doi.org/10.1021/ic100063c

Bonhote P, Moser JE, Humphry-Baker R, Vlachopoulos N, Zakeeruddin SM, Walder L, Gratzel M (1999) Long-lived photoinduced charge separation and redox-type photochromism on mesoporous oxide films sensitized by molecular dyads. J Am Chem Soc 121:1324–1336. https://doi.org/10.1021/ja981742j

Byrne A, Burke CS, Keyes TE (2016) Precision targeted ruthenium(ii) luminophores; highly effective probes for cell imaging by stimulated emission depletion (STED) microscopy. Chem Sci 7:6551–6562. https://doi.org/10.1039/c6sc02588a

Caramori S, Cristino V, Argazzi R, Meda L, Bignozzi CA (2010) Photoelectrochemical behavior of sensitized TiO(2) photoanodes in an aqueous environment: application to hydrogen production. Inorg Chem 49:3320–3328. https://doi.org/10.1021/ic9023037

Carreno A et al (2016a) Theoretical and experimental characterization of a novel pyridine benzimidazole: suitability for fluorescence staining in cells and antimicrobial properties. New J Chem 40:2362–2375. https://doi.org/10.1039/c5nj02772a

Carreno A et al (2016b) Fluorescence probes for prokaryotic and eukaryotic cells using Re(CO)(3)(+) complexes with an electron withdrawing ancillary ligand. New J Chem 40:7687–7700. https://doi.org/10.1039/c6nj00905k

Carreno A et al (2019) Cyclic voltammetry, relativistic DFT calculations and biological test of cytotoxicity in walled-cell models of two classical rhenium (I) tricarbonyl complexes with 5-amine-1,10-phenanthroline. Chem Phys Lett 715:231–238. https://doi.org/10.1016/j.cplett.2018.11.043

Carreño A, Aros AE, Otero C, Polanco R, Gacitúa M, Arratia-Pérez R, Fuentes JA (2017a) Substituted bidentate and ancillary ligands modulate the bioimaging properties of the classical Re(i) tricarbonyl core with yeasts and bacteria. New J Chem 41:2140–2147. https://doi.org/10.1039/c6nj03792e

Carreño A, Gacitúa M, Molins E, Arratia-Pérez R (2017b) X-ray diffraction and relativistic DFT studies on the molecular biomarker fac-Re(CO)3(4,4′-dimethyl-2,2′-bpy)(E-2-((3-amino-pyridin-4-ylimino)-methyl)-4,6-di-tert-butylphenol)(PF6). Chem Pap 71:2011–2022. https://doi.org/10.1007/s11696-017-0196-6

Casida M (2009) Time-dependent density-functional theory for molecules and molecular solids. J Mol Struct (Thoechem) 914:3–18. https://doi.org/10.1016/j.theochem.2009.08.018

Caveney NA, Li FK, Strynadka NC (2018) Enzyme structures of the bacterial peptidoglycan and wall teichoic acid biogenesis pathways. Curr Opin Struct Biol 53:45–58. https://doi.org/10.1016/j.sbi.2018.05.002

Chaves GM, da Silva WP (2012) Superoxide dismutases and glutaredoxins have a distinct role in the response of *Candida albicans* to oxidative stress generated by the chemical compounds

menadione and diamide. Mem I Oswaldo Cruz 107:998–1005. https://doi.org/10.1590/S0074-02762012000800006

Cuenca-Estrella M et al (2003) Multicenter evaluation of the reproducibility of the proposed antifungal susceptibility testing method for fermentative yeasts of the Antifungal Susceptibility Testing Subcommittee of the European Committee on Antimicrobial Susceptibility Testing (AFST-EUCAST). Clin Microbiol Infect 9:467–474

de Menorval MA, Mir LM, Fernandez ML, Reigada R (2012) Effects of dimethyl sulfoxide in cholesterol-containing lipid membranes: a comparative study of experiments in silico and with cells. PLoS ONE 7:e41733. https://doi.org/10.1371/journal.pone.0041733

Donnici CL et al (1998) Synthesis of the novel 4,4′- and 6,6′-dihydroxamic-2,2′-bipyridines and improved routes to 4,4′- and 6,6′- substituted 2,2′-bipyridines and mono-*N*-oxide-2,2′-bipyridine. J Braz Chem Soc 9:1. https://doi.org/10.1590/s0103-50531998000500008

Dreyse P, Loeb B, Soto-Arriaza M, Tordera D, Orti E, Serrano-Perez JJ, Bolink HJ (2013) Effect of free rotation in polypyridinic ligands of Ru(II) complexes applied in light-emitting electrochemical cells. Dalton Trans 42:15502–15513. https://doi.org/10.1039/c3dt52067f

Fantacci S, De Angelis F, Sgamellotti A, Marrone A, Re N (2005) Photophysical properties of $[Ru(phen)_2(dppz)]^{2+}$ intercalated into DNA: an integrated Car-Parrinello and TDDFT study. J Am Chem Soc 127:14144–14145. https://doi.org/10.1021/ja054368d

Farnum BH, Jou JJ, Meyer GJ (2012) Visible light generation of I-I bonds by Ru-tris(diimine) excited states. Proc Natl Acad Sci USA 109:15628–15633. https://doi.org/10.1073/pnas.1118340109

Favereau L et al (2016) A molecular tetrad that generates a high-energy charge-separated state by mimicking the photosynthetic Z-scheme. J Am Chem Soc 138:3752–3760. https://doi.org/10.1021/jacs.5b12650

Franco de Carvalho F, Pignedoli CA, Tavernelli I (2017) TDDFT-based spin-orbit couplings of 0D, 1D, and 2D carbon nanostructures: static and dynamical effects. J Phys Chem C 121:10140–10152. https://doi.org/10.1021/acs.jpcc.7b00331

Gajardo F, Barrera M, Vargas R, Crivelli I, Loeb B (2011) Influence of the nature of the absorption band on the potential performance of high molar extinction coefficient ruthenium(II) polypyridinic complexes as dyes for sensitized solar cells. Inorg Chem 50:5910–5924. https://doi.org/10.1021/ic1020862

Gow NAR, Latge JP, Munro CA (2017) The fungal cell wall: structure, biosynthesis, and function. Microbiol Spectr. https://doi.org/10.1128/microbiolspec.FUNK-0035-2016

Grotjahn R, Maier TM, Michl J, Kaupp M (2017) Development of a TDDFT-based protocol with local hybrid functionals for the screening of potential singlet fission chromophores. J Chem Theory Comput 13:4984–4996. https://doi.org/10.1021/acs.jctc.7b00699

Juris A, Balzani V, Barigelletti F, Campagna S, Belser P, von Zelewsky A (1988) Ru(II) polypyridine complexes: photophysics, photochemistry, eletrochemistry, and chemiluminescence. Coordin Chem Rev 84:85–277. https://doi.org/10.1016/0010-8545(88)80032-8

Katsumata K, Matsui H, Yamaguchi T, Tanabe N (2017) 6-(2-Quinolinyl)-2,2′-bipyridine ruthenium complexes for near-infrared sensitization in dye-sensitized solar cells. Inorg Chim Acta 463:118–125. https://doi.org/10.1016/j.ica.2017.04.030

Kendall K, Roberts AD (2015) van der Waals forces influencing adhesion of cells Philosophical transactions of the Royal Society of London Series B. Biol Sci 370:20140078. https://doi.org/10.1098/rstb.2014.0078

Koyyada G et al (2016) New terpyridine-based ruthenium complexes for dye sensitized solar cells applications. Inorg Chim Acta 442:158–166. https://doi.org/10.1016/j.ica.2015.11.031

León-García MC, Ríos-Castro E, López-Romero E, Cuéllar-Cruz M (2017) Evaluation of cell wall damage by dimethyl sulfoxide in *Candida* species. Res Microbiol 168:732–739. https://doi.org/10.1016/j.resmic.2017.06.001

Li HF, Zhang LS, Lin H, Fan XL (2014) A DFT-D study on the electronic and photophysical properties of ruthenium(II) complex with a chelating sulfoxide group. Chem Phys Lett 604:10–14. https://doi.org/10.1016/j.cplett.2014.04.048

Li X, Gorle AK, Ainsworth TD, Heimann K, Woodward CE, Collins JG, Keene FR (2015) RNA and DNA binding of inert oligonuclear ruthenium(II) complexes in live eukaryotic cells. Dalton Trans 44:3594–3603. https://doi.org/10.1039/c4dt02575j

Macleod-Carey D, Caramori GF, Guajardo-Maturana R, Paez-Hernandez D, Muñoz-Castro A, Arratia-Perez R (2018) Advances in bonding and properties of inorganic systems from relativistic calculations in Latin. Am Int J Quant Chem. https://doi.org/10.1002/qua.25777

Micciarelli M, Curchod BFE, Bonella S, Altucci C, Valadan M, Rothlisberger U, Tavernelli I (2017) Characterization of the photochemical properties of 5-benzyluracil via time-dependent density functional theory. J Phys Chem A 121:3909–3917. https://doi.org/10.1021/acs.jpca.6b12799

Muñoz-Castro A, Páez-Hernández D, Arratia-Pérez R (2017) Spin-orbit effect into isomerization barrier of small gold Clusters. $O_h \leftrightarrow D_{2h}$ Fluxionality of the Au_6^{2+} cluster Investigated by relativistic methods. Chem Phys Lett 683:404–407. https://doi.org/10.1016/j.cplett.2017.02.054

Nazeeruddin MK et al (2001) Engineering of efficient panchromatic sensitizers for nanocrystalline TiO_2-based solar cells. J Am Chem Soc 123:1613–1624. https://doi.org/10.1021/ja003299u

Nir S, Andersen M (1977) Van der Waals interactions between cell surfaces. J Membr Biol 31:1–18

Oßwald S, Breimaier S, Linseis M, Winter RF (2017) Polyelectrochromic vinyl ruthenium-modified tritylium dyes. Organometallics 36:1993–2003. https://doi.org/10.1021/acs.organomet.7b00194

Páez-Hernández D, Murillo-López JA, Arratia-Pérez R (2012) Optical and magnetic properties of the complex bis(dicyclooctatetraenyl) diuranium. A Theoretical View Organometallics 31:6297–6304. https://doi.org/10.1021/om300560h

Poynton FE, Bright SA, Blasco S, Williams DC, Kelly JM, Gunnlaugsson T (2017) The development of ruthenium(ii) polypyridyl complexes and conjugates for in vitro cellular and in vivo applications. Chem Soc Rev 46:7706–7756. https://doi.org/10.1039/c7cs00680b

Rojas-Poblete M, Carreño A, Gacitúa M, Páez-Hernández D, Rabanal-Leon WA, Arratia-Pérez R (2018) Electrochemical behaviors and relativistic DFT calculations to understand the terminal ligand influence on the $[Re_6(\mu_3\text{-}Q)_8X_6]^{4-}$ clusters. New J Chem 42:5471–5478. https://doi.org/10.1039/C7NJ05114J

Rowe RK, Ho PS (2017) Relationships between hydrogen bonds and halogen bonds in biological systems. Acta Crystallogr B Struct Sci Cryst Eng Mater 73:255–264. https://doi.org/10.1107/S2052520617003109

Sacksteder L, Zipp AP, Brown EA, Streich J, Demas JN, Degraff BA (1990) Luminescence studies of pyridine alpha-diimine rhenium(I) tricarbonyl complexes. Inorg Chem 29:4335–4340. https://doi.org/10.1021/ic00346a033

Sampaio RN, Muller AV, Polo AS, Meyer GJ (2017) Correlation between charge recombination and lateral hole-hopping kinetics in a series of *cis*-Ru(phen')(dcb)$(NCS)_2$ dye-sensitized solar cells ACS. Appl Mater Interfaces 9:33446–33454. https://doi.org/10.1021/acsami.7b01542

Sangilipandi S, Sutradhar D, Bhattacharjee K, Kaminsky W, Joshi SR, Chandra AK, Mohan Rao K (2016) Synthesis, structure, antibacterial studies and DFT calculations of arene ruthenium, Cp*Rh, Cp*Ir and tricarbonylrhenium metal complexes containing

2-chloro-3-(3-(2-pyridyl)pyrazolyl)quinoxaline ligand. Inorg Chim Acta 441:95–108. https://doi.org/10.1016/j.ica.2015.11.012

Sanz AB, Garcia R, Rodriguez-Pena JM, Arroyo J (2017) The CWI Pathway: regulation of the transcriptional adaptive response to cell wall stress in yeast. J Fungi (Basel). https://doi.org/10.3390/jof4010001

Sauvage JP et al (1994) Ruthenium(II) and osmium(II) bis(terpyridine) complexes in covalently-linked multicomponent systems—synthesis, electrochemical-behavior, absorption-spectra, and photochemical and photophysical properties. Chem Rev 94:993–1019. https://doi.org/10.1021/cr00028a006

Schatzschneider U (2018) Metallointercalators and metalloinsertors: structural requirements for DNA recognition and anticancer activity. Met Ions Life Sci. https://doi.org/10.1515/9783110470734-020

Sinnecker S, Rajendran A, Klamt A, Diedenhofen M, Neese F (2006) Calculation of solvent shifts on electronic g-tensors with the conductor-like screening model (COSMO) and its self-consistent generalization to real solvents (direct COSMO-RS). J Phys Chem A 110:2235–2245. https://doi.org/10.1021/jp056016z

Sistla YS, Khanna A (2011) Validation and prediction of the temperature-dependent Henry's constant for CO_2–ionic liquid systems using the conductor-like screening model for realistic solvation (COSMO-RS). J Chem Eng Data 56:4045–4060. https://doi.org/10.1021/je200486c

Song HW et al (2017) Ultrafast relaxation dynamics of amine-substituted bipyridyl ruthenium(II) complexes. Chem Phys Lett 683:322–328. https://doi.org/10.1016/j.cplett.2017.03.017

Tsai KY, Chang IJ (2017) Oxidation of bromide to bromine by ruthenium(II) bipyridine-type complexes using the flash-quench technique. Inorg Chem 56:8497–8503. https://doi.org/10.1021/acs.inorgchem.7b01238

Van Kuiken BE et al (2013) Simulating Ru L_3-edge X-ray absorption spectroscopy with time-dependent density functional theory: model complexes and electron localization in mixed-valence metal dimers. J Phys Chem A 117:4444–4454. https://doi.org/10.1021/jp401020j

Wang W, Zhang J, Wang H, Chen L, Bian Z (2016) Photocatalytic and electrocatalytic reduction of CO_2 to methanol by the homogeneous pyridine-based systems. Appl Catal A 520:1–6. https://doi.org/10.1016/j.apcata.2016.04.003

Weerawardene KLDM, Aikens CM (2018) Origin of Photoluminescence of Ag25(SR)18—nanoparticles: ligand and doping effect. J Phys Chem C 122:2440–2447. https://doi.org/10.1021/acs.jpcc.7b11706

Westwater C, Balish E, Schofield DA (2005) *Candida albicans*-conditioned medium protects yeast cells from oxidative stress: a possible link between quorum sensing and oxidative stress resistance. Eukaryot Cell 4:1654–1661. https://doi.org/10.1128/EC.4.10.1654-1661.2005

Wu Q et al (2018) Rigid dinuclear ruthenium-arene complexes showing strong DNA interactions. J Inorg Biochem 189:30–39. https://doi.org/10.1016/j.jinorgbio.2018.08.013

Yadav AK, Espaillat A, Cava F (2018) Bacterial strategies to preserve cell wall integrity against environmental threats. Front Microbiol 9:2064. https://doi.org/10.3389/fmicb.2018.02064

Yang G, Guan W, Yan L, Su Z, Xu L, Wang EB (2006) Theoretical study on the electronic spectrum and the origin of remarkably large third-order nonlinear optical properties of organoimide derivatives of hexamolybdates. J Phys Chem B 110:23092–23098. https://doi.org/10.1021/jp062820p

Younker JM, Dobbs KD (2013) Correlating experimental photophysical properties of iridium(III) complexes to spin-orbit coupled TDDFT predictions. J Phys Chem C 117:25714–25723. https://doi.org/10.1021/jp410576a

Zalis S, Lam YC, Gray HB, Vlcek A (2015) Spin-orbit TDDFT electronic structure of diplatinum(II, II) complexes. Inorg Chem 54:3491–3500. https://doi.org/10.1021/acs.inorgchem.5b00063

Zarate X, Schott E, Gomez T, Arratia-Perez R (2013) Theoretical study of sensitizer candidates for dye-sensitized solar cells: peripheral substituted dizinc pyrazinoporphyrazine-phthalocyanine complexes. J Phys Chem A 117:430–438. https://doi.org/10.1021/jp3067316

Zhong YW, Wu SH, Burkhardt SE, Yao CJ, Abruna HD (2011) Mononuclear and dinuclear ruthenium complexes of 2,3-Di-2-pyridyl-5,6-diphenylpyrazine: synthesis and spectroscopic and electrochemical studies. Inorg Chem 50:517–524. https://doi.org/10.1021/ic101629w

Zhou M, Robertson GP, Roovers J (2005) Comparative study of ruthenium(II) tris(bipyridine) derivatives for electrochemiluminescence application. Inorg Chem 44:8317–8325. https://doi.org/10.1021/ic0510112